Quantum Algorithms for Fermionic Quantum Field Theories

Stephen P. Jordan,[†] Keith S. M. Lee,[‡♯] and John Preskill [§] [*]

[†] *National Institute of Standards and Technology, Gaithersburg, MD, USA*

[‡] *Perimeter Institute for Theoretical Physics, Waterloo, ON, Canada*

[♯] *Institute for Quantum Computing and Department of Physics & Astronomy,*
University of Waterloo, Waterloo, ON, Canada

[§] *Institute for Quantum Information and Matter,*
California Institute of Technology, Pasadena, CA, USA

Abstract

Extending previous work on scalar field theories, we develop a quantum algorithm to compute relativistic scattering amplitudes in fermionic field theories, exemplified by the massive Gross-Neveu model, a theory in two spacetime dimensions with quartic interactions. The algorithm introduces new techniques to meet the additional challenges posed by the characteristics of fermionic fields, and its run time is polynomial in the desired precision and the energy. Thus, it constitutes further progress towards an efficient quantum algorithm for simulating the Standard Model of particle physics.

---

[*]stephen.jordan@nist.gov, ksml@theory.caltech.edu, preskill@theory.caltech.edu

1 Introduction

Whether a universal quantum computer is sufficiently powerful to be able to perform quantum field-theoretical computations efficiently has been a long-standing and important open question. Efficient quantum algorithms for simulating quantum many-body systems have been developed theoretically [1–3] and implemented experimentally [4–6], but quantum field theory presents additional technical challenges, such as the formally infinite number of degrees of freedom per unit volume. In earlier work [7,8], we presented and analyzed a quantum algorithm for simulating a bosonic quantum field theory called ϕ^4 theory. That algorithm runs in a time that is polynomial in the number of particles, their energy, and the desired precision, and applies at both weak and strong coupling. Hence, it offers exponential speedup over existing classical methods at high precision or strong coupling. In this paper, we extend our work to fermionic quantum field theories, exemplified by the massive Gross-Neveu model, a theory in two spacetime dimensions with quartic interactions. Although our analysis is specific to this theory, our algorithm can be adapted to other massive fermionic quantum field theories with only minor modification while retaining polynomial complexity.

Our quantum algorithm generates scattering events: it takes (as the input) the momenta of the incoming particles and, sampling from the probability distribution of possible outcomes, returns (as the output) the momenta of the outgoing particles produced by the physical scattering process. Physical quantities of interest, such as scattering cross sections, can thus be approximated by repeated runs of the simulation, together with statistical data analysis similar to that used for particle-accelerator experiments.

The features of fermionic field theories not present in bosonic theories pose new technical problems, the solutions to which require different techniques. Perhaps the most obvious difference is the anticommutation, rather than commutation, of fermionic fields. This forces a change in the representation of the state by qubits: we use an encoding method for fermionic mode occupation numbers introduced by Bravyi and Kitaev [9]. In [8], it was shown that simulation of Hamiltonian time evolution via Suzuki-Trotter formulae has efficiency advantages when applied to spatially local Hamiltonians. Fermionic anticommutation makes it more difficult to gain efficiency by exploiting spatial locality. Nevertheless, we obtain a construction that gives quasi-linear asymptotic scaling in time and the number of lattice sites, as in the bosonic case.

In contrast with bosonic field theories, discretization of fermionic field theories leads to the well-known "fermion doubling" problem, in which spurious fermion species not in the continuum theory appear in the discretized theory. One solution used in lattice gauge theory is to add to the action the so-called Wilson term, a second-derivative operator that vanishes in the naive continuum limit. The Wilson term can also be accommodated in our quantum algorithm; in particular, we show how it can be turned on during the preparation of the ground state.

In general, state preparation is a demanding task. The algorithm in [7, 8] uses a three-step procedure. First, the free vacuum is prepared. For the free scalar theory, this is a multivariate Gaussian wavefunction. Next, wavepackets are excited within the free theory. In order that only single-particle states are created, an ancillary qubit is used, together with a particular Hamiltonian that acts on the enlarged space. Finally, the interaction is turned on via a generalization of adiabatic state preparation that can be applied to superpositions of eigenstates. This procedure intersperses backwards time evolutions governed by time-independent Hamiltonians into the turn-on to undo the different dynamical phases, which otherwise would cause undesirable propagation and broadening of wavepackets.

The state-preparation method analyzed here differs from that of [7,8] in two main ways. Prepa-

ration of the free vacuum requires modification because the vacuum of the free fermionic theory is different from that of the free bosonic theory. For this purpose, we incorporate a separate adiabatic turn-on step. Furthermore, sources are used to create particle excitations after the coupling constant is adiabatically turned on, rather than before. (This difference is not required by the fermionic nature of the theory.) This method has the advantage that it works when bound states are possible, in which case the adiabatic wavepacket preparation of [7,8] might fail. Another consequence is that the procedure no longer requires the interleaving of backwards time evolutions to undo dynamical phases. On the other hand, a disadvantage is that the preparation of each particle has a significant probability of producing no particle. In the case of two-particle scattering, one can perform additional repetitions of the simulation, and recognize and discard simulations in which fewer than two particles have been created. However, the procedure is not well suited to processes involving more than two incoming particles.

We analyze two different measurement procedures to be used as the last step of the simulation. The first method is to return adiabatically to the free theory and then measure the number operators of the momentum modes. For unbound states, this procedure yields complete information about particle momenta, but is not well-suited to detecting bound states or resolving spatial information. The second procedure is to measure charge within local regions of space. These measurements can detect charged bound states, although they are blind to neutral ones. Which of these measurement schemes is preferable depends on the desired application.

There is a substantial body of work on analog quantum simulation of quantum systems, including lattice field theories. (See [10] for a recent review.) In such work, proposals are made for the engineering of experimental systems so that they mimic systems of interest, that is, so that the Hamiltonians of the laboratory systems approximate Hamiltonians of interest. The proposed quantum simulators can be thought of as specialized quantum computers. In contrast, we address digital quantum algorithms, namely, algorithms to be run on a universal, fault-tolerant, digital quantum computer. Our work thus probes the fundamental asymptotic computational complexity of quantum field theories.

There is also an extensive literature on the study of quantum field theories on classical computers via lattice field theory. (See Ch. 17 of [11] for a review of its results and status.) However, classical lattice algorithms rely on analytic continuation to imaginary time, $t \to -i\tau$. Thus, they are useful for computing static quantities such as mass ratios, but are unsuitable for calculating dynamical quantities such as scattering cross sections. In contrast, our quantum algorithm simulates the dynamics of quantum field theories, a problem that is expected to be BQP-complete and thus impossible to solve by polynomial-time classical algorithms. Although our algorithm draws upon some concepts from lattice field theory, new techniques are needed, particularly for state preparation and measurement.

The work presented in this paper is another step towards the goal of obtaining an efficient quantum algorithm for simulating the Standard Model of particle physics. Such an algorithm would establish that, except for quantum-gravity effects, the standard quantum circuit model suffices to capture completely the computational power of our universe.

The rest of this paper is organized as follows. Section 2 introduces the massive Gross-Neveu model, gives an overview of our quantum algorithm for computing the theory's scattering amplitudes, and analyzes the algorithm's complexity. Section 3 describes in detail the efficient simulation of the Hamiltonian time evolution in the quantum circuit model. Section 4 presents our procedures for state preparation and measurement. Finally, Section 5 addresses some field-theoretical aspects,

3

namely, the effects of a non-zero lattice spacing and the renormalization of mass, which are crucial elements in our complexity analysis.

2 Quantum Algorithm

In this section we describe the massive Gross-Neveu model (§2.1), outline the steps in our algorithm for simulating particle scattering processes within this model (§2.2), and give an overview of the algorithm's complexity (§2.3). The run time is polynomial in the inverse of the desired precision and in the momenta of the incoming particles. The detailed analysis of the steps of the algorithm that contribute to the overall complexity stated in §2.3 is given in later sections.

2.1 The Massive Gross-Neveu Model

The theory we consider is a generalization of the Gross-Neveu model to include an explicit mass term in the Lagrangian. The (original) Gross-Neveu model [12] is a quantum field theory in two spacetime dimensions consisting of N fermion species with quartic interactions. It has a rich phenomenology. Like quantum chromodynamics (QCD), the theory governing the strong interactions, it has the remarkable property of asymptotic freedom, whereby the interaction becomes weaker at higher energies. The theory has a discrete chiral symmetry, $\psi \to \gamma^5 \psi$, where

$$\gamma^5 = \begin{bmatrix} 1 & 0 \\ 0 & -1 \end{bmatrix}. \tag{1}$$

This symmetry is spontaneously broken by the non-perturbative vacuum. (The related theory known as the chiral Gross-Neveu model has a continuous chiral symmetry, $\psi \to e^{i\theta\gamma^5}\psi$.) Correspondingly, mass is generated dynamically, and the theory admits a topological soliton, the Callan-Coleman-Gross-Zee (CCGZ) kink. Non-topological solitons also exist [13].

These interesting characteristics have attracted intense study and led to applications not only in particle physics but also in condensed-matter physics, including studies of ferromagnetic superconductors [14], conducting polymers, and systems of strongly correlated electrons [15].

The Gross-Neveu model, together with the chiral Gross-Neveu model, was originally solved in the limit $N \to \infty$ [12]. Via inverse scattering methods [16], and later through a generalized Bethe Ansatz [17], integrability was demonstrated for general values of N, a feature related to the existence of infinitely many conserved currents [18]. The model's S-matrix is factorizable [19, 20]: the n-body S-matrix is expressible as the product of two-body S-matrices.

In contrast, the massive Gross-Neveu model, in which there is an explicit bare mass, is thought not to be integrable for arbitrary values of N. This theory still exhibits asymptotic freedom, but it does not admit solitons: for any non-zero mass, the CCGZ kink becomes infinitely massive and disappears [21]. The asymptotic freedom and non-zero bare mass make a rigorous perturbative construction of the theory satisfying the Osterwalder-Schrader axioms possible [22, 23].

The massive N-component Gross-Neveu model is given by the following Lagrangian in two spacetime dimensions:

$$\mathcal{L} = \sum_{j=1}^{N} \bar{\psi}_j (i\gamma^\mu \partial_\mu - m)\psi_j + \frac{g^2}{2}\left(\sum_{j=1}^{N} \bar{\psi}_j \psi_j\right)^2, \tag{2}$$

4

where each field $\psi_j(x)$ has two components, γ^μ is a two-dimensional representation of the Dirac algebra, and $\bar{\psi} = \psi^\dagger \gamma^0$.[1] We use the Majorana representation, namely,

$$\gamma^0 = \begin{bmatrix} 0 & -i \\ i & 0 \end{bmatrix}, \qquad \gamma^1 = -\begin{bmatrix} 0 & i \\ i & 0 \end{bmatrix}. \tag{3}$$

The components of the field operator associated with the particle species $j \in \{1, 2, \ldots, N\}$ will be denoted by $\psi_{j,\alpha}$, $\alpha \in \{0, 1\}$. In units where $\hbar = c = 1$, any quantity has units of some power of mass, referred to as the mass dimension. We shall use bold-face to represent spatial vectors, such as $\mathbf{p}$ and $\mathbf{x}$, to distinguish them from spacetime vectors $x^\mu = (t, \mathbf{x})$ and $p^\mu = (E, \mathbf{p})$. Note, however, that we are considering 1+1 dimensions; thus, spatial vectors have only one component.

The dimensionless parameter g determines the strength of the interaction. When $g = 0$, the ψ_j are free fields obeying the Dirac equation, $(i\gamma^\mu \partial_\mu - m_0)\psi_j(x) = 0$. Then one can write

$$\psi_j(x) = \int \frac{d\mathbf{p}}{2\pi} \frac{1}{\sqrt{2E_\mathbf{p}}} \left(a_j(\mathbf{p})u(\mathbf{p})e^{-ip\cdot x} + b_j^\dagger(\mathbf{p})v(\mathbf{p})e^{ip\cdot x} \right), \tag{4}$$

where

$$E_\mathbf{p} = \sqrt{\mathbf{p}^2 + m_0^2}, \tag{5}$$

$a_j(\mathbf{p})$, $b_j^\dagger(\mathbf{p})$ are creation and annihilation operators, and u, v satisfy

$$(m_0\gamma^0 + \mathbf{p}\gamma^0\gamma^1)u(\mathbf{p}) = E_\mathbf{p}u(\mathbf{p}), \tag{6}$$

$$(m_0\gamma^0 - \mathbf{p}\gamma^0\gamma^1)v(\mathbf{p}) = -E_\mathbf{p}v(\mathbf{p}), \tag{7}$$

$$u^\dagger(\mathbf{p})u(\mathbf{p}) = v^\dagger(\mathbf{p})v(\mathbf{p}) = 2E_\mathbf{p}, \tag{8}$$

$$u(\mathbf{p})^\dagger v(-\mathbf{p}) = 0, \tag{9}$$

$$\bar{u}(\mathbf{p})u(\mathbf{p}) = -\bar{v}(\mathbf{p})v(\mathbf{p}) = 2m_0, \tag{10}$$

$$\bar{u}(\mathbf{p})v(\mathbf{p}) = \bar{v}(\mathbf{p})u(\mathbf{p}) = 0. \tag{11}$$

In the Majorana representation (3), one has the following concrete solution:

$$u(\mathbf{p}) = \begin{bmatrix} \sqrt{E_\mathbf{p} - \mathbf{p}} \\ i\sqrt{E_\mathbf{p} + \mathbf{p}} \end{bmatrix}, \qquad v(\mathbf{p}) = \begin{bmatrix} \sqrt{E_\mathbf{p} - \mathbf{p}} \\ -i\sqrt{E_\mathbf{p} + \mathbf{p}} \end{bmatrix}. \tag{12}$$

2.2 Description of Algorithm

To represent the field using qubits, we first discretize the quantum field theory, putting it on a spatial lattice. (Discretization errors are analyzed in §5.1.) Having done that, our algorithm consists of six main steps, which we analyze in subsequent sections.

1. Prepare the ground state of the Hamiltonian with both the interaction term (g_0^2) and the nearest-neighbor lattice-site interactions turned off. This can be done efficiently because the ground state is a tensor product of the ground states of the individual lattice sites.

2. Simulate, via Suzuki-Trotter formulae, the adiabatic turn-on of the nearest-neighbor lattice-site interactions, thereby obtaining the ground state of the non-interacting theory.

---

[1] The Dirac matrices satisfy $\{\gamma^\mu, \gamma^\nu\} \equiv \gamma^\mu\gamma^\nu + \gamma^\nu\gamma^\mu = 2g^{\mu\nu}\mathbb{1}$, and $\psi_j(x)$ is a spinor, that is, its Lorentz transformation is such that (2) is Lorentz-invariant. We use the metric $g^{\mu,\nu} = \mathrm{diag}(+1, -1)$.

3. Adiabatically turn on the interaction term, while adjusting the parameter m_0 to compensate for the renormalization of the physical mass.

4. Excite particle wavepackets, by introducing a source term in the Hamiltonian. The source term is chosen to be sinusoidally varying in time and space so as to select the desired mass and momentum of particle excitations by resonance.

5. Evolve in time, via Suzuki-Trotter formulae, according to the full massive Gross-Neveu Hamiltonian. It is during this time evolution that scattering may occur.

6. Either use phase estimation to measure local charge observables, or adiabatically return to the free theory and then use phase estimation to measure number operators of momentum modes. (The choice between these forms of measurement depends on the application.)

2.3 Complexity

In this section we bound the asymptotic scaling of the number of gates needed to simulate scattering processes as a function of the momentum p of the incoming particles and the precision ϵ to which the final results are desired. The effect of discretization, via a lattice of spacing a, is captured by (infinitely many) terms in the effective Hamiltonian that are not present in the continuum massive Gross-Neveu theory (§5.1). Truncation of these terms, which make contributions of $O(a)$ to scattering cross sections, therefore constitutes an error. Thus, to ensure any cross section σ' in the discretized quantum field theory matches the continuum value σ to within

$$(1 - \epsilon)\sigma \leq \sigma' \leq (1 + \epsilon)\sigma, \tag{13}$$

one must choose the scaling $a \sim \epsilon$ in the high-precision limit, that is, the limit $\epsilon \to 0$. Similarly, in the large-momentum limit, one must choose the scaling $a \sim p^{-1}$ in order to ensure that the wavelength of each particle is large compared with the lattice spacing.

It suffices to use an adiabatic process of duration

$$T = O\left(\frac{L^2}{a^4 m^3 \epsilon}\right) \tag{14}$$

(where L is the length of the spatial dimension and m is the physical mass) to prepare a state within a distance ϵ of the free vacuum (§4.1). Using Suzuki-Trotter decompositions of the form described in §3.3, we can simulate this adiabatic time evolution using a number of quantum gates scaling as

$$G_{\text{prep}} = O\left(\left(\frac{TL}{a^2}\right)^{1+o(1)} \epsilon^{-o(1)}\right) \tag{15}$$

$$= O\left(\left(\frac{L^3}{a^6 m^3 \epsilon}\right)^{1+o(1)}\right). \tag{16}$$

The next state-preparation step is to simulate adiabatic turn-on of the coupling, thereby obtaining the interacting vacuum. This can be achieved in a time (§4.2)

$$T_{\text{turn-on}} = O\left(\frac{L^2}{a^4 m^3 \epsilon}\right). \tag{17}$$

Applying Suzuki-Trotter formulae, one obtains a gate count of

$$G_{\text{turn-on}} = O\left(\left(\frac{L^3}{a^6 m^3 \epsilon}\right)^{1+o(1)}\right). \tag{18}$$

The final state-preparation step is to excite particle wavepackets. We do this by applying a time-dependent perturbation $\lambda W(t)$ for time τ. It is necessary to choose τ large enough and λ small enough to suppress the production of particle pairs. The choice of small λ means that there will be a substantial probability that no particle is produced. Let p_1 denote the probability that exactly one particle is produced. In a typical simulation one wishes to produce an initial state of two spatially separated incoming particles. The probability that both of these are produced is p_1^2. The simulations in which one or both initial particles has failed to be created can be detected at the final measurement stage of the simulation and discarded. This comes at the cost of a factor of $1/p_1^2$ more repetitions of the simulation. The probability p_1 is independent of momentum and scales with precision as $p_1 \sim \epsilon$ (§4.3). Also, in §4.3 one finds that the total number of quantum gates needed for the excitation step is

$$G_{\text{excite}} = \begin{cases} \epsilon^{-4-o(1)}, & \text{as } \epsilon \to 0, \\ p^{3+o(1)}, & \text{as } p \to \infty. \end{cases} \tag{19}$$

In both the high-momentum and high-precision limits, the dominant costs in the algorithm are the two adiabatic state preparation steps, whose complexity is given in (16) and (18). In the high-precision limit, to compute physical quantities such as scattering cross sections to within a factor of $(1+\epsilon)$, one must choose a to scale as ϵ (§5.1). Also, in this limit, the complexity contains a further factor of $1/\epsilon$ owing to postselection of simulations in which both wavepacket excitations have been successful (§4.3). Substituting $a \sim \epsilon$ into (16) and including this extra factor of $1/\epsilon$ yield a total complexity of $O(\epsilon^{-8-o(1)})$. In the high-momentum limit, a must scale as $1/p$ to ensure that the particle wavelength is long compared to the lattice spacing, and L must scale as p to accommodate the excitation step (§4.3). In summary, we obtain

$$G_{\text{total}} = \begin{cases} O(\epsilon^{-8-o(1)}), & \text{as } \epsilon \to 0, \\ O(p^{9+o(1)}), & \text{as } p \to \infty. \end{cases} \tag{20}$$

Note that these are only upper bounds on the complexity, and it may be possible to improve them by using more detailed analysis, such as more specialized adiabatic theorems.

3   Qubits and Quantum Gates

We divide the problem of simulating Hamiltonian time evolutions in the massive Gross-Neveu model into three subproblems. The first subproblem is to represent the state of the field with qubits. We do this by choosing a complete set of commuting observables and encoding their eigenvalues with strings of bits (§3.1). The second subproblem is to simulate local fermionic gates on the degrees of freedom defined by the commuting observables. Achieving this in an efficient manner is non-trivial because of the fermionic statistics. For this purpose, we employ a technique due to Bravyi and Kitaev [9], which implements fermionic statistics with only logarithmic overhead in the number of lattice sites (§3.2). The third subproblem is to decompose the time evolution governed by the

massive Gross-Neveu Hamiltonian into a product of local fermionic gates. We do this using high-order Suzuki-Trotter formulae [24] with optimizations tailored to the fermionic statistics and the spatially local nature of the Hamiltonian (§3.3). The local unitary transformations act on at most 2^{2N}-dimensional Hilbert spaces and can therefore be efficiently decomposed into elementary gates for any constant number of particle species, N, via the Solovay-Kitaev algorithm [25, 26].

3.1   Representation by Qubits

First, we put the massive Gross-Neveu model on a spatial lattice

$$\Omega = a\mathbb{Z}_{\hat{L}} \, . \tag{21}$$

For simplicity, we impose periodic boundary conditions, so that Ω can be considered a circle of circumference $L = a\hat{L}$. The Hamiltonian is

$$H = H_0 + H_g + H_W \, , \tag{22}$$

where

$$H_0 \;=\; \sum_{\mathbf{x}\in\Omega} a \sum_{j=1}^{N} \bar{\psi}_j(\mathbf{x})\left[-i\gamma^1\frac{\psi_j(\mathbf{x}+a)-\psi_j(\mathbf{x}-a)}{2a} + m_0\psi_j(\mathbf{x})\right] \, , \tag{23}$$

$$H_g \;=\; -\frac{g_0^2}{2}\sum_{\mathbf{x}\in\Omega} a\left(\sum_{j=1}^{N}\bar{\psi}_j(\mathbf{x})\psi_j(\mathbf{x})\right)^2 \, , \tag{24}$$

$$H_W \;=\; \sum_{\mathbf{x}\in\Omega} a \sum_{j=1}^{N}\left[-\frac{r}{2a}\bar{\psi}_j(\mathbf{x})\left(\psi_j(\mathbf{x}+a) - 2\psi_j(\mathbf{x}) + \psi_j(\mathbf{x}-a)\right)\right] \, . \tag{25}$$

Here, H_g is the interaction term, and H_W is the Wilson term, used to prevent fermion doubling [27]. Correspondingly, $0 < r \leq 1$ is called the Wilson parameter. H is spatially local in the sense that it consists only of single-site and nearest-neighbor terms on the lattice.

Let Γ denote the momentum-space lattice corresponding to Ω, namely,

$$\Gamma = \frac{2\pi}{L}\mathbb{Z}_{\hat{L}} \, . \tag{26}$$

We can deduce the spectrum $H_0 + H_W$ using

$$\psi_j(\mathbf{x}) \;=\; \sum_{\mathbf{p}\in\Gamma}\frac{1}{L}\frac{1}{\sqrt{2E_{\mathbf{p}}}}\left(a_j(\mathbf{p})u(\mathbf{p})e^{i\mathbf{p}\cdot\mathbf{x}} + b_j^\dagger(\mathbf{p})v(\mathbf{p})e^{-i\mathbf{p}\cdot\mathbf{x}}\right) \, , \tag{27}$$

$$\bar{\psi}_j(\mathbf{x}) \;=\; \sum_{\mathbf{p}\in\Gamma}\frac{1}{L}\frac{1}{\sqrt{2E_{\mathbf{p}}}}\left(a_j^\dagger(\mathbf{p})\bar{u}(\mathbf{p})e^{-i\mathbf{p}\cdot\mathbf{x}} + b_j(\mathbf{p})\bar{v}(\mathbf{p})e^{i\mathbf{p}\cdot\mathbf{x}}\right) \, . \tag{28}$$

The inverse transformation is

$$a_j(\mathbf{p}) \;=\; \frac{1}{\sqrt{2E_{\mathbf{p}}}}u^\dagger(\mathbf{p})\sum_{\mathbf{x}\in\Omega} a e^{-i\mathbf{p}\cdot\mathbf{x}}\psi_j(\mathbf{x}) \, , \tag{29}$$

$$b_j^\dagger(\mathbf{p}) \;=\; \frac{1}{\sqrt{2E_{\mathbf{p}}}}v^\dagger(\mathbf{p})\sum_{\mathbf{x}\in\Omega} a e^{i\mathbf{p}\cdot\mathbf{x}}\psi_j(\mathbf{x}) \, . \tag{30}$$

8

Substituting (27) and (28) into (23) and (25) and neglecting the vacuum energy, we obtain

$$H_0 + H_W = \sum_{j=1}^{N} \sum_{\mathbf{p} \in \Gamma} \frac{1}{L} E_{\mathbf{p}}^{(a)}(m_0) \left(a_j^\dagger(\mathbf{p}) a_j(\mathbf{p}) + b_j^\dagger(\mathbf{p}) b_j(\mathbf{p}) \right) , \tag{31}$$

where

$$E_{\mathbf{p}}^{(a)}(m_0) = \sqrt{\left(m_0 + \frac{2r}{a} \sin^2 \left(\frac{\mathbf{p}a}{2} \right) \right)^2 + \frac{1}{a^2} \sin^2(\mathbf{p}a)} . \tag{32}$$

From the canonical fermionic anticommutation relations

$$\{\psi_{j,\alpha}(\mathbf{x}), \psi_{k,\beta}^\dagger(\mathbf{y})\} = a^{-1} \delta_{\mathbf{x},\mathbf{y}} \delta_{j,k} \delta_{\alpha,\beta} \mathbb{1} , \tag{33}$$

$$\{\psi_{j,\alpha}^\dagger(\mathbf{x}), \psi_{k,\beta}^\dagger(\mathbf{y})\} = \{\psi_{j,\alpha}(\mathbf{x}), \psi_{k,\beta}(\mathbf{y})\} = 0 , \tag{34}$$

it follows that

$$\{a_j(\mathbf{p}), a_k^\dagger(\mathbf{q})\} = L \delta_{\mathbf{p},\mathbf{q}} \delta_{j,k} \mathbb{1} , \tag{35}$$

$$\{b_j(\mathbf{p}), b_k^\dagger(\mathbf{q})\} = L \delta_{\mathbf{p},\mathbf{q}} \delta_{j,k} \mathbb{1} , \tag{36}$$

with all other anticommutators involving a and b operators equal to zero. We thus have the following interpretation: there are N independent fermion species, created (with momentum $\mathbf{p}$) by $a_1^\dagger(\mathbf{p}), \ldots, a_N^\dagger(\mathbf{p})$ and annihilated by $a_1(\mathbf{p}), \ldots, a_N(\mathbf{p})$. Similarly, for each species j, $b_j^\dagger(\mathbf{p})$ and $b_j(\mathbf{p})$ are the creation and annihilation operators for a corresponding antifermion. Thus, H acts on a Hilbert space of dimension $2^{2N\hat{L}}$.

We can specify a basis for the Hilbert space of field states by choosing a complete set of commuting observables. The basis is then indexed by the set of eigenvalues of these observables. The fermionic anticommutation relations $\{a, a^\dagger\} = \mathbb{1}$, $\{a, a\} = 0$ imply that the algebra generated by a and $a^\dagger$ has the irreducible representation $a \to \begin{bmatrix} 0 & 1 \\ 0 & 0 \end{bmatrix}$, $a^\dagger \to \begin{bmatrix} 0 & 0 \\ 1 & 0 \end{bmatrix}$, which is unique up to the choice of basis. Hence, the eigenvalues of $a^\dagger a$ are 0 and 1. The two basis vectors for the space on which a and $a^\dagger$ act are interpreted as the presence or absence of a fermion.

Thus, by (33) and (34),

$$S_x = \{a \psi_{j,\alpha}^\dagger(\mathbf{x}) \psi_{j,\alpha}(\mathbf{x}) | j = 1, \ldots, N; \ \alpha = 0, 1; \ \mathbf{x} \in \Omega\} \tag{37}$$

is a set of $2N\hat{L}$ commuting observables, each of which has eigenvalues zero and one. Similarly, by (35) and (36),

$$S_p = \{L^{-1} a_j^\dagger(\mathbf{p}) a_j(\mathbf{p}) | j = 1, \ldots, N; \ \mathbf{p} \in \Gamma\} \cup \{L^{-1} b_j^\dagger(\mathbf{p}) b_j(\mathbf{p}) | j = 1, \ldots, N; \ \mathbf{p} \in \Gamma\} \tag{38}$$

is a set of $2N\hat{L}$ commuting observables, each with eigenvalues zero and one. In the non-interacting theory, the eigenvalues of the elements of S_p are interpreted as the fermionic occupation numbers of different momentum modes.

The Hamiltonian $H_0 + H_W$ is called the free theory. The eigenstates of the number operators in S_p are eigenstates of $H_0 + H_W$, and thus the particles do not interact. The rest mass of these non-interacting particles is $E_0^{(a)}(m_0) = m_0$. It is not known how to solve for the spectrum of

9

$H_0 + H_W + H_g$ analytically, but the eigenvalue spectrum of $H_0 + H_W + H_g$ can still be characterized in terms of particles. The rest mass m of the particles in $H_0 + H_W + H_g$ is equal to the eigenvalue gap between the ground state (also called the vacuum) and the first excited state. In the interacting theory, it is no longer true that $m = m_0$. Rather, m depends in a non-trivial way on m_0, g_0, and a; the mass is said to be renormalized. A quantitative analysis of this effect contributes to our analysis of adiabatic state preparation and is given in §5.2.

One can represent the quantum state of the fermionic fields using $2N\hat{L}$ qubits to store the eigenvalues of the elements of either S_x or S_p. The ground state of the free theory in the S_p representation is thus $|000\ldots\rangle$. However, the ground state of the interacting theory is non-trivial in both representations. We define our qubit basis in terms of the elements of S_x, because the Gross-Neveu Hamiltonian is local in this basis, which improves the scaling of the Suzuki-Trotter formulae used to implement time evolution. However, we do not simply store the eigenvalues of the elements of S_x directly as the values of the qubits. This representation would be somewhat inefficient to act upon, because direct implementation of the fermionic minus signs requires $O(\hat{L})$ gates. Instead, we apply the method of [9] to reduce this overhead to $O(\log \hat{L})$, as described next.

3.2 Simulating Fermionic Gates

The implementation of fermionic gates using qubits can present a technical challenge [9]. As an example, consider the unitary transformation $U_{j,\alpha}(\mathbf{x}) = \sqrt{a}\big(\psi_{j,\alpha}(\mathbf{x}) + \psi^\dagger_{j,\alpha}(\mathbf{x})\big)$. This toggles the eigenvalue of $a\psi_{j,\alpha}(\mathbf{x})\psi^\dagger_{j,\alpha}(\mathbf{x})$ between zero and one. Such a toggling can be implemented on qubits with the NOT gate. However, to satisfy the fermionic anticommutation relations (33) and (34) the sign of the transition amplitude between the zero and one state must depend on the occupation of other modes. A well-known way to satisfy (33) and (34) is to use a Jordan-Wigner transformation, in which the modes are given an ordering and $U_{j,\alpha}(\mathbf{x})$ is represented by the operator $\sigma_x \otimes \sigma_z \otimes \ldots \otimes \sigma_z$, where the σ_z operators apply to all preceding modes[2] [28]. Unfortunately, this method clearly has an $O(\hat{L})$ overhead. In [9], Bravyi and Kitaev give a method with only $O(\log \hat{L})$ overhead, which we briefly review here.

Let n_i be the occupation number of the ith fermionic mode according to some chosen numbering of the modes from 1 to $2N\hat{L}$. To implement the minus signs in $U_{j,\alpha}(\mathbf{x})$, one needs to know $\sum_i n_i$, where the sum is over all preceding modes. Thus, a natural encoding of fermionic mode occupation numbers is to store the quantities $t_i = \sum_{j=1}^{i} n_j$ instead of the quantities n_i. This encoding has the advantage that calculating the relevant signs has an $O(1)$ cost. However, it has the disadvantage that, if the occupation number of the ith mode changes, then $i-1$ of the t_i values must be updated. Thus, updates have an $O(\hat{L})$ cost. The Bravyi-Kitaev encoding uses the following compromise, in which the calculation of the relevant signs and the update steps can both be performed in time $O(\log \hat{L})$.

The mode index $i \in \{1, \ldots, 2N\hat{L}\}$ can be represented by a bit string of length $l = \lceil \log_2(2N\hat{L}) \rceil$. One can define the following partial order on these bit strings. Consider two bit strings $x = x_l x_{l-1} \ldots x_1$ and $y = y_l y_{l-1} \ldots y_1$. Then $x \preceq y$ if, for some r, $x_j = y_j$ for $j > r$ and $y_{r-1} = y_{r-2} = \ldots = y_1 = 1$. Now, let $k_j = \sum_{s \preceq j} n_s$. Any total occupation number t_i can be computed from the k_j quantities in $O(\log \hat{L})$ time and changing the occupation of any mode n_j requires updating only $O(\log \hat{L})$ of the k_j quantities [9].

---

[2]Note that one can apply both the Jordan-Wigner and Bravyi-Kitaev methods for implementing fermionic operators on quantum computers in any number of spatial dimensions, using an arbitrary numbering of modes.

In fact, the Bravyi-Kitaev construction is relevant only to the excitation of wavepackets (§4.3). In all other parts of our algorithm, we simulate a Hamiltonian in which every term is a product of an even number of fermionic field operators, all acting on the same site or on nearest-neighbor sites in one dimension. In this case, traditional Jordan-Wigner techniques incur only $O(1)$ overhead.

3.3 Application of Suzuki-Trotter Formulae to Fermionic systems

In this section, we describe how to construct efficient quantum circuits that simulate time evolution induced by the Hamiltonian H defined in (22), (23), (24), and (25). We present the case in which H is time-independent. By the results of [29], the same analysis applies to the simulation of the time-dependent Hamiltonians that we use in adiabatic state preparation. (See also [30].)

Using a kth-order Suzuki-Trotter formula, one can implement Hamiltonian time evolution of duration t using a number of quantum gates that scales as $t^{1+\frac{1}{2k}}$ [24, 31]. Generally, applying a Suzuki-Trotter formula directly to a Hamiltonian of the form

$$H = \sum_{i=1}^{m} H_i \tag{39}$$

yields an algorithm with $O(m^{1+o(1)})$ timesteps, and hence $O(m^{2+o(1)})$ gates, if the H_i are not mutually commuting. Thus, it is often advantageous to group terms in a Hamiltonian like (39) into as small a collection as possible of sets of mutually commuting terms [8, 32].

Consider the problem of simulating the Hamiltonian H defined in (22), (23), (24), and (25). By (33) and (34), one sees that

$$[\bar{\psi}_j(\mathbf{x})\psi_j(\mathbf{x}), \bar{\psi}_k(\mathbf{y})\psi_k(\mathbf{y})] = 0 \,, \tag{40}$$

regardless of whether $j = k$ or $\mathbf{x} = \mathbf{y}$. Thus, we start by decomposing H as a sum of two parts, the single-site terms and the terms that couple nearest neighbors:

$$H = H_{\text{ss}} + H_{\text{nn}} \,, \tag{41}$$

where

$$H_{\text{ss}} = \sum_{\mathbf{x}\in\Omega} a \left[\sum_{j=1}^{N} \left(m_0 \bar{\psi}_j(\mathbf{x})\psi_j(\mathbf{x}) + \frac{r}{a}\bar{\psi}_j(\mathbf{x})\psi_j(\mathbf{x}) \right) + \frac{g_0^2}{2} \left(\sum_{j=1}^{N} \bar{\psi}_j(\mathbf{x})\psi_j(\mathbf{x}) \right)^2 \right] . \tag{42}$$

By (40), $e^{-iH_{\text{ss}}\delta t}$ decomposes into a product of local unitary transformations.

All terms in H_{nn} are of the form

$$\psi_{j,\alpha}^{\dagger}(\mathbf{x})\psi_{j,\beta}(\mathbf{y}) + \psi_{j,\beta}^{\dagger}(\mathbf{y})\psi_{j,\alpha}(\mathbf{x}) \,, \tag{43}$$

for $\mathbf{x} = \mathbf{y} \pm a$. Terms with $\alpha = \beta$ and terms with $\alpha \neq \beta$ are both present in H_{nn}.

Given an operator of the form (43), let us refer to the subset of $\{1, \ldots, N\} \times \{0, 1\} \times \Omega$ on which it acts as its support. Because they consist of a product of an even number of fermionic operators, any two operators of the form (43) commute provided they have disjoint support. Thus, we next decompose H_{nn} as

$$H_{\text{nn}} = H_1 + H_2 + H_3 + H_4 \,, \tag{44}$$

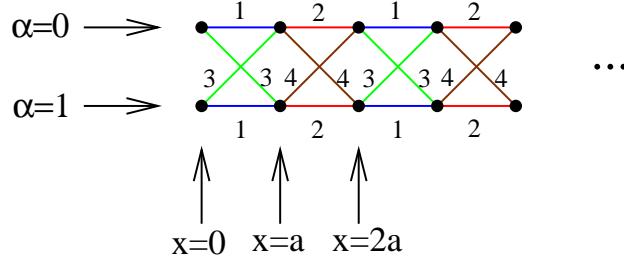where each of $H_1, \ldots, H_4$ consists of a sum of terms with non-intersecting support.

Figure 1: Vertices represent elements of $\{0,1\} \times \Omega$ two vertices are connected by an edge if H_{nn} couples these sites. (Different species are never coupled by H_{nn}, so the full graph with vertices corresponding to elements of $\{1,\ldots,N\} \times \{0,1\} \times \Omega$ would consist of N disconnected copies of the graph shown.) The edges can be colored with four colors such that each node has no more than one incident edge of each color. One can obtain the decomposition $H_{\mathrm{nn}} = H_1 + H_2 + H_3 + H_4$ by choosing H_1 to be the sum of all interaction terms along the edges labeled 1 (which are blue), H_2 to be the sum of all the interaction terms along edges labeled 2 (which are red), and so on.

In H_{nn} there is no coupling between different species, that is, no products of ψ_j and ψ_k for $j \neq k$. Thus, we can ignore the index j. We now construct a graph whose vertices correspond to the elements of $\{0,1\} \times \Omega$. We draw an edge between two vertices if there exists a term in H_{nn} with the corresponding support. One sees that this graph is as shown in Fig. 1. The graph is edge-colorable with four colors, and therefore H_{nn} is correspondingly decomposable as in (44) with each of H_1, H_2, H_3, H_4 consisting of a sum of commuting terms. (Because of the periodic boundary conditions, this works only if $\hat{L}$ is even, which we assume henceforth.)

The unitary time evolution induced by $H = H_{\mathrm{ss}} + H_1 + H_2 + H_3 + H_4$ can be approximately decomposed via high-order Suzuki-Trotter formulae into a sequence of

$$n_{\mathrm{S-T}} = O\big((t/a)^{1+o(1)} \hat{L}^{o(1)} \epsilon^{-o(1)}\big) \tag{45}$$

time evolutions induced by individual members of $\{H_{\mathrm{ss}}, H_1, H_2, H_3, H_4\}$. The scaling with t follows from [24, 29]. The scaling with $\hat{L}$ is a consequence of the spatial locality of H (see §4.3 of [8]), that is, the property that only nearest-neighbor sites are coupled. The scaling with a is a consequence of the fact that the individual terms in the Hamiltonian each have norm at most of order a^{-1}. This affects the magnitude of the error term in the Suzuki-Trotter decomposition, which arises from commutators of these terms.

Each member of $\{H_{\mathrm{ss}}, H_1, H_2, H_3, H_4\}$ is a sum of $O(\hat{L})$ commuting terms. The time evolution $e^{-i \sum_i M_i t}$ induced by commuting terms M_i decomposes as $e^{-i \sum_i M_i t} = \prod_i e^{-i M_i t}$. If each H_i acts on only a constant number of qubits, then the individual factors $e^{-i H_i t}$ in this product can each be simulated in $\widetilde{O}(1)$ time, by the Solovay-Kitaev theorem [25, 26]. Thus, including a logarithmic overhead for fermionic statistics, the cost of implementing $e^{-i J t}$ for any $J \in \{H_{\mathrm{ss}}, H_1, H_2, H_3, H_4\}$ is $\widetilde{O}(\hat{L})$. By (45), the total cost of time evolution is $O\big(\big(\frac{tL}{a^2}\big)^{1+o(1)} \epsilon^{-o(1)}\big)$ quantum gates.

4 State Preparation and Measurement

We divide the problem of state preparation into three steps, described in §4.1–§4.3: preparing the free vacuum, transforming the free vacuum into the interacting vacuum, and exciting wavepackets

on the background of the interacting vacuum. Two possible measurement procedures are described in §4.4 and §4.5.

4.1 Preparing the Free Vacuum

Although the free Hamiltonian $H_0 + H_W$ is exactly solvable, preparing its ground state in the S_x representation on a quantum computer is non-trivial. We do so using adiabatic state preparation, as follows. Let

$$H(s) = \sum_{\mathbf{x} \in \Omega} a \sum_{j=1}^{N} \bar{\psi}_j(\mathbf{x}) \left[-si\gamma^1 \frac{\psi_j(\mathbf{x}+a) - \psi_j(\mathbf{x}-a)}{2a} + m\psi_j(\mathbf{x}) \right] + sH_W. \tag{46}$$

The energy gap of this Hamiltonian is equal to the parameter m for all s. We set this equal to the physical mass of the particles whose scattering we ultimately wish to simulate.

$H(0)$ is a sum of separate Hamiltonians acting on each lattice site and each species of particle. Its ground state is therefore the tensor product of the ground states of the four-dimensional Hilbert spaces associated with each pair $(\mathbf{x}, j) \in \Omega \times \{1, \ldots, N\}$. (Specifically, the ground state for a given site is $\frac{1}{\sqrt{2}} (|01\rangle + i|10\rangle)$, where $|b_0 b_1\rangle$ with $b_0, b_1 \in \{0, 1\}$ denotes the state satisfying $a\psi_{j,0}^\dagger(\mathbf{x})\psi_{j,0}(\mathbf{x})|b_0 b_1\rangle = b_0|b_0 b_1\rangle$ and $a\psi_{j,1}^\dagger(\mathbf{x})\psi_{j,1}(\mathbf{x})|b_0 b_1\rangle = b_1|b_0 b_1\rangle$.) The cost of producing this tensor product of $N\hat{L}$ local states, including the cost of fermionic antisymmetrization via the encoding of [9], is $O(N\hat{L} \log(N\hat{L}))$.

After the ground state of H_0 has been prepared, the complexity of the remaining adiabatic state preparation is determined by the adiabatic theorem [33, 34].

Theorem 1. *Let $H(s)$ be a finite-dimensional twice differentiable Hamiltonian on $0 \leq s \leq 1$ with a non-degenerate ground state $|\phi_0(s)\rangle$ separated by an energy gap $\gamma(s)$. Let $|\psi(t)\rangle$ be the state obtained by Schrödinger time evolution according to the Hamiltonian $H(t/T)$ from the state $|\phi_0(0)\rangle$ at $t = 0$. Then, with an appropriate choice of phase for $|\phi_0(t)\rangle$, the error $\Delta \equiv \| |\psi(T)\rangle - |\phi_0(1)\rangle \|$ satisfies*

$$\Delta \leq \frac{1}{T} \left[\frac{1}{\gamma(0)^2} \left\| \frac{\mathrm{d}H}{\mathrm{d}s} \right\|_{s=0} + \frac{1}{\gamma(1)^2} \left\| \frac{\mathrm{d}H}{\mathrm{d}s} \right\|_{s=1} + \int_0^1 \mathrm{d}s \left(\frac{5}{\gamma^3} \left\| \frac{\mathrm{d}H}{\mathrm{d}s} \right\|^2 + \frac{1}{\gamma^2} \left\| \frac{\mathrm{d}^2 H}{\mathrm{d}s^2} \right\| \right) \right]. \tag{47}$$

Analyzing the adiabaticity of this process is relatively easy, because (27) and (28) diagonalize $H(s)$ (and $\frac{dH}{ds}$) for all s. One finds that the eigenvalue gap of $H(s)$ throughout the adiabatic path $0 \leq s \leq 1$ is always precisely m. Furthermore,

$$\frac{dH}{ds} = \sum_{j=1}^{N} \sum_{\mathbf{p} \in \Gamma} \frac{1}{L} E_{\mathbf{p}}^{(a)}(0) \left(a_j^\dagger(\mathbf{p})a_j(\mathbf{p}) + b_j^\dagger(\mathbf{p})b_j(\mathbf{p}) \right). \tag{48}$$

Thus,

$$\left\| \frac{dH}{ds} \right\| = 2N \sum_{\mathbf{p} \in \Gamma} E_{\mathbf{p}}^{(a)}(0). \tag{49}$$

13

For large L, $\sum_{\mathbf{p} \in \Gamma} \frac{1}{L}$ becomes well approximated by the integral $\int_0^{2\pi/a} d\mathbf{p}$. Thus, using (32), we obtain

$$\left\| \frac{dH}{ds} \right\| \simeq 2NL \int_0^{2\pi/a} d\mathbf{p} E_{\mathbf{p}}^{(a)}(0) \tag{50}$$

$$= 2NL \int_0^{2\pi/a} d\mathbf{p} \sqrt{\frac{4r^2}{a^2} \sin^4\left(\frac{\mathbf{p}a}{2}\right) + \frac{1}{a^2} \sin^2(\mathbf{p}a)} \tag{51}$$

$$= \frac{2NL}{a^2} \eta(r), \tag{52}$$

where

$$\eta(r) = \int_0^{2\pi} d\hat{p} \sqrt{4r^2 \sin^4\left(\frac{\hat{p}}{2}\right) + \sin^2(\hat{p})}. \tag{53}$$

We can therefore substitute $\frac{d^2 H}{ds^2} = 0$, $\left\| \frac{dH}{ds} \right\| = O(La^{-2})$ and $\gamma = m$ into (47). Theorem 1 then shows that we can prepare a state with distance no more than ϵ_{prep} from the exact state using

$$T = O\left(\frac{L^2}{a^4 m^3 \epsilon_{\text{prep}}}\right). \tag{54}$$

Note that the adiabatic theorem applied here, though convenient because of its generality, may not yield a tight upper bound on the run time.

4.2   Preparing the Interacting Vacuum

Given the ground state of the free theory, we can prepare the ground state of the interacting theory by adiabatically varying the parameters g_0^2 and m_0 in the massive Gross-Neveu Hamiltonian, starting from $g_0^2 = 0$. For adiabaticity to be maintained, the physical mass must not vanish at any point in the adiabatic path. By §5.2, the physical mass varies with g_0^2 according to

$$m = m_0 - c_1 g_0^2 - c_2 g_0^4 + O(g_0^6), \tag{55}$$

where $c_1, c_2 > 0$ are given by

$$c_1 = \frac{m}{2\pi} \log\left(\frac{1}{ma}\right) + \cdots, \tag{56}$$

$$c_2 \simeq \frac{m}{16\pi^3} (9.3N - 0.07) \log^2(ma) + \cdots. \tag{57}$$

(The coefficients in (57) were determined numerically.) The vanishing of the physical mass marks the location of a quantum phase transition, which cannot be adiabatically crossed. Equation (55) indicates that the phase diagram takes the schematic form as shown in Fig. 2.

As in §4.1, we parametrize our adiabatic state preparation by a quantity s, which increases over time from 0 to 1. In this second adiabatic process, the Hamiltonian is the full massive Gross-Neveu Hamiltonian with s-dependent parameters $g_0^2(s)$ and $m_0(s)$. We choose $g_0^2(0) = 0$ and $m_0(0) = m$ so that the initial Hamiltonian of this adiabatic process matches the final Hamiltonian of the preceding adiabatic step. Thus, the ground state at $s = 0$ is the free vacuum prepared in the previous step of the algorithm. To keep our analysis simple, we choose a linear adiabatic path, namely,

$$g_0^2(s) = s g_0^2,$$
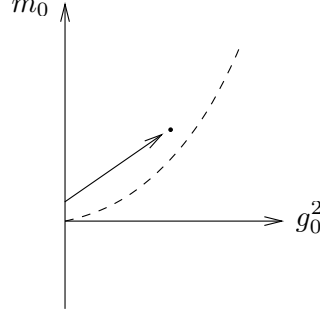$$m_0(s) = m + s \delta_m. \tag{58}$$

14

Figure 2: Our perturbative calculations of the physical mass in the massive Gross-Neveu model indicate a phase diagram with the qualitative features illustrated above. The phase above the dashed curve is accessible adiabatically from the free theory but the phase below is not. The arrow depicts our linear adiabatic path, described in (59). Our perturbative analysis shows that the first two derivatives of the phase transition curve with respect to g_0^2 are both positive and diverge only as $\text{poly}(\log(m_0 a))$ in the limit $a \to 0$.

We choose δ_m so that the physical mass at $s = 1$ is equal to the physical mass at $s = 0$. To second order in g_0^2,

$$\delta_m = c_1 g_0^2 + c_2 g_0^4 + \cdots , \tag{59}$$

as illustrated in Fig. 2.

By (58), $\frac{d^2 H}{ds^2} = 0$ and

$$\frac{dH}{ds} = \sum_{\mathbf{x} \in \Omega} a \left[\delta_m \bar{\psi}_j(\mathbf{x}) \psi_j(\mathbf{x}) + \frac{g_0^2}{2} \left(\sum_{j=1}^{N} \bar{\psi}_j(\mathbf{x}) \psi_j(\mathbf{x}) \right)^2 \right] . \tag{60}$$

Furthermore, the minimal eigenvalue gaps occur at $s = 0$ and $s = 1$ and are equal to the final physical mass m. Thus, to apply Theorem 1 we need only bound $\left\| \frac{dH}{ds} \right\|$.

We can deduce the spectrum of $\frac{dH}{ds}$ by the following transformation:

$$a_j(\mathbf{x}) = \frac{1}{\sqrt{2}} \left(\psi_{j,0}(\mathbf{x}) - i\psi_{j,1}(\mathbf{x}) \right) , \tag{61}$$

$$b_j^\dagger(\mathbf{x}) = \frac{1}{\sqrt{2}} \left(\psi_{j,0}(\mathbf{x}) + i\psi_{j,1}(\mathbf{x}) \right) . \tag{62}$$

This corresponds to

$$\psi_j(\mathbf{x}) = \frac{1}{\sqrt{2m_0}} \left(a_j(\mathbf{x}) u(0) + b_j^\dagger(\mathbf{x}) v(0) \right) , \tag{63}$$

where u, v are defined in (12). Using (33) and (34), one can verify that

$$\{a_j(\mathbf{x}), a_k^\dagger(\mathbf{y})\} = \{b_j(\mathbf{x}), b_k^\dagger(\mathbf{y})\} = a^{-1} \delta_{j,k} \delta_{\mathbf{x},\mathbf{y}} \mathbb{1} , \tag{64}$$

$$\{a_j(\mathbf{x}), a_k(\mathbf{y})\} = \{b_j(\mathbf{x}), b_k(\mathbf{y})\} = 0 , \tag{65}$$

$$\{a_j(\mathbf{x}), b_k(\mathbf{y})\} = \{a_j^\dagger(\mathbf{x}), b_k(\mathbf{y})\} = 0 . \tag{66}$$

Thus, $a_j(\mathbf{x}), a_j^\dagger(\mathbf{x}), b_j(\mathbf{x}), b_j^\dagger(\mathbf{x})$ are creation and annihilation operators for $2N$ species of fermions localized on the spatial lattice. By (63),

$$\bar{\psi}_j(\mathbf{x}) \psi_j(\mathbf{x}) = a_j^\dagger(\mathbf{x}) a_j(\mathbf{x}) - b_j(\mathbf{x}) b_j^\dagger(\mathbf{x}) , \tag{67}$$

15

from which we obtain

$$\left\| \sum_{j=1}^{N} \bar{\psi}_j(\mathbf{x}) \psi_j(\mathbf{x}) \right\| = 2Na^{-1}, \tag{68}$$

and hence

$$\left\| \frac{dH}{ds} \right\| = \delta_m 2N\hat{L} + \frac{2\hat{L}g_0^2 N^2}{a}. \tag{69}$$

By the results of §5.2, we find that $\delta_m = O(\log^2(ma))$. Hence, recalling that $\hat{L} = L/a$, we obtain

$$\left\| \frac{dH}{ds} \right\| = O\left(\frac{L}{a^2} \right). \tag{70}$$

Therefore, by Theorem 1 the diabatic error is at most

$$\epsilon = O\left(\frac{1}{T_{\text{turn-on}}} \frac{\left\| \frac{dH}{ds} \right\|^2}{\gamma^3} \right) \tag{71}$$

$$= O\left(\frac{L^2}{T_{\text{turn-on}} a^4 m^3} \right). \tag{72}$$

It thus suffices to choose

$$T_{\text{turn-on}} = O\left(\frac{L^2}{a^4 \epsilon m^3} \right). \tag{73}$$

In the above procedure, we choose our adiabatic path so that the initial and final physical masses equal some user-specified value m. To achieve this, one needs to tune the quantity δ_m in accordance with (58) and (59). For sufficiently weak coupling, the proper choice of δ_m can be determined by the perturbative calculations performed in §5.2. In the strongly coupled case, these perturbative calculations no longer provide precise guidance as to a choice of δ_m. Instead, as previously discussed in [8], the adiabatic path can be determined by the quantum computer. Specifically, one can measure the physical mass at a given coupling strength g_0 by exciting a particle and measuring energy via phase estimation. This measurement guides the choice of a suitable adiabatic path to a slightly larger coupling strength, at which point the mass can be measured again. Iterating this process, one can reach any coupling strength for which the corresponding vacuum is in the same quantum phase as the free vacuum.

4.3 Exciting Wavepackets

After preparing the interacting vacuum, $|\text{vac}\rangle$, we excite wavepackets by simulating a source that varies sinusoidally in space and time so as to induce excitations of some particular total energy and momentum by resonance. Given the physical rest mass m of the particles, we can choose this energy and momentum so that the only corresponding state is a single-particle state. (For a given total momentum, an unbound state of two particles will have greater energy than the corresponding state of one particle. In the ultrarelativistic limit, $p \gg m$, this energy difference scales as m^2/p.) In the remainder of this section, we show that, using a source of spatial extent l and duration τ, one can ensure that excitations off resonance are suppressed as $\sim \exp\left[-\frac{1}{4}\left(l^2(\mathbf{p} - \mathbf{p}_0)^2 + \tau^2(E - E_0)^2 \right) \right]$. Hence, by simulating a process of duration $\tau \sim p/m^2$ and spatial extent $l \sim p/m^2$, one can control the incoming momentum and ensure that the probability of obtaining more than one particle is small.

16

The creation of two incoming particles has only an $O(\epsilon)$ success probability, which can be compensated for by repeated attempts. (See the discussion following (82).) The total complexity of preparing two particles is the cost of simulating the time evolution given in (75) a total of $1/\epsilon$ times. Thus, by the results of §3.3, the complexity is $\left(\frac{\tau l}{a^2 \epsilon}\right)^{1+o(1)}$. Thus, since $p \sim a^{-1}$ for fixed ϵ and $a \sim \epsilon$ for fixed p, the number of quantum gates G_{excite} needed to excite the two initial particles is

$$G_{\text{excite}} \sim \begin{cases} \epsilon^{-3-o(1)}, & \text{as } \epsilon \to 0, \\ p^{4+o(1)}, & \text{as } p \to \infty. \end{cases} \tag{74}$$

Note also that for the initial wavepackets to be well separated, L must be larger than $2l$. Hence, in the high-momentum limit $L \sim p$, which affects the complexity of other steps of the algorithm.

Perturbative Expansion

The resonant excitation can be analyzed with time-dependent perturbation theory. Let

$$R = T\left\{\exp\left[-i\int_0^\tau \mathrm{d}t\,(H + \lambda W(t))\right]\right\}, \tag{75}$$

where $T\{\cdot\}$ denotes the time-ordered product, H is given by (22),

$$W(t) = \int \mathrm{d}\mathbf{x}\,\left(f(t,\mathbf{x})\psi_{i,\alpha}(\mathbf{x}) + f^*(t,\mathbf{x})\psi_{i,\alpha}^\dagger(\mathbf{x})\right), \tag{76}$$

i and α are chosen according to the desired type of particle, and $f(t,\mathbf{x})$ is an oscillatory function whose form we optimize in the next subsection. The end product of the excitation process is $R|\text{vac}\rangle$. One can expand this quantity using the Dyson series, as follows:

$$R = \mathbb{1} - i\lambda \int_0^\tau \mathrm{d}t_1 W_I(t_1) + (-i\lambda)^2 \int_0^\tau \mathrm{d}t_1 \int_0^{t_1} \mathrm{d}t_2 W_I(t_1)W_I(t_2) + \cdots, \tag{77}$$

where

$$W_I(t) = e^{iHt}W(t)e^{-iHt} \tag{78}$$

and the nth-order term in λ is

$$(-i\lambda)^n \int_0^\tau \mathrm{d}t_1 \ldots \int_0^{t_{n-1}} \mathrm{d}t_n W_I(t_1)\ldots W_I(t_n). \tag{79}$$

The total contribution from orders λ^2 and higher is bounded by

$$\left\| \sum_{n=2}^\infty (-i\lambda)^n \int_0^\tau \mathrm{d}t_1 \ldots \int_0^{t_{n-1}} \mathrm{d}t_n W_I(t_1)\ldots W_I(t_n) \right\| \leq \sum_{n=2}^\infty \frac{\lambda^n \tau^n}{n!} w^n \tag{80}$$

$$= \exp[\lambda\tau w] - 1 - \lambda\tau w, \tag{81}$$

where

$$w = \max_{0 \leq t \leq \tau} \|W(t)\|. \tag{82}$$

From the above analysis, one sees that the Dyson series converges rapidly. The single-particle excitation amplitude is of order λ, and the dominant error, other than non-excitation, is the two-particle excitation amplitude, which is of order λ^2. Setting the two-particle excitation probability

to ϵ, one obtains a single-particle excitation with probability $p_1 \sim \sqrt{\epsilon}$, and non-excitation with probability on the order of $1 - \sqrt{\epsilon}$. In a standard scattering simulation, one wishes to prepare as an initial state single-particle excitations at two spatially separated locations. The fraction of simulations in which this is achieved (rather than one or both particles failing to be produced) is thus of order $p_1^2 \sim \epsilon$. One can detect such instances and compensate by repeating the simulation $O(1/p_1^2)$ times and postselecting the instances in which both particles were produced.

Next, we consider the first-order excitation amplitude in more detail. Let $|E, \mathbf{p}\rangle$ be any state with total momentum $\mathbf{p}$ and energy E above the vacuum energy, so that $P|E, \mathbf{p}\rangle = \mathbf{p}|E, \mathbf{p}\rangle$ and $H|E, \mathbf{p}\rangle = E|E, \mathbf{p}\rangle$, where P is the total momentum operator. (Here, we rely on the fact that $[H, P] = 0$.) Then, to first order in λ, by (77) and (78),

$$\langle E, \mathbf{p}|R|\text{vac}\rangle \simeq -i\lambda \int_0^\tau dt \langle E, \mathbf{p}|W_I(t)|\text{vac}\rangle \tag{83}$$

$$= -i\lambda \int_0^\tau dt\, e^{-iEt} \langle E, \mathbf{p}|W(t)|\text{vac}\rangle. \tag{84}$$

Recalling that the momentum operator is the generator of spatial translations, one has $\psi_{i,\alpha}(\mathbf{x}) = e^{iP\mathbf{x}}\psi_{i,\alpha}(0)e^{-iP\mathbf{x}}$. Thus, to first order in λ,

$$\langle E, \mathbf{p}|R|\text{vac}\rangle \simeq -i\lambda \int_0^\tau dt \int d\mathbf{x} e^{-i(Et + \mathbf{p}\mathbf{x})} \left[f(t, \mathbf{x})\langle E, \mathbf{p}|\psi_{i,\alpha}(0)|\text{vac}\rangle + f^*(t, \mathbf{x})\langle E, \mathbf{p}|\psi_{i,\alpha}^\dagger(0)|\text{vac}\rangle \right]. \tag{85}$$

(Here we have used $P|\text{vac}\rangle = 0$.) Defining $f(t, \mathbf{x}) = 0$ for $t \notin [0, \tau]$, we can extend the time integration to infinity and express $\langle E, \mathbf{p}|R|\text{vac}\rangle$ in terms of $\tilde{f}$, the Fourier transform of f. For our choice of f, given in the next subsection, $\tilde{f}$ is real, and therefore

$$\langle E, \mathbf{p}|R|\text{vac}\rangle = -i\lambda \left[\tilde{f}(E, \mathbf{p})\langle E, \mathbf{p}|\psi_{i,\alpha}(0)|\text{vac}\rangle + \tilde{f}(-E, -\mathbf{p})\langle E, \mathbf{p}|\psi_{i,\alpha}^\dagger(0)|\text{vac}\rangle \right] + O(\lambda^2). \tag{86}$$

Wavepacket Shaping

We now show that a Gaussian wavepacket is a good choice for $f(t, \mathbf{x})$. Specifically, for chosen constants $\alpha, \beta > 0$, let

$$f(t, \mathbf{x}) = \begin{cases} \eta \exp\left[-(\alpha t)^2 - (\beta \mathbf{x})^2 - iE_0 t + i\mathbf{p}_0\mathbf{x}\right], & -\tau/2 \leq t \leq \tau/2, -l/2 \leq \mathbf{x} \leq l/2, \\ 0, & \text{otherwise}. \end{cases} \tag{87}$$

(For convenience, we have shifted the origin of the coordinate system.) Here η is a normalization factor[3] with mass dimension $3/2$. With this choice of f,

$$\tilde{f}(E, \mathbf{p}) = \eta q_{\beta,l}(\mathbf{p} - \mathbf{p}_0)q_{\alpha,\tau}(E - E_0), \tag{88}$$

where

$$q_{\rho,r}(d) = \int_{-r/2}^{r/2} d\mathbf{x}\, e^{id\mathbf{x} - (\rho\mathbf{x})^2}. \tag{89}$$

---

[3]It is reasonable to choose η so that $\int_0^\tau dt W_I(t)|\text{vac}\rangle$ is a normalized state. In the ultrarelativistic limit this implies that $\eta \sim \left(\alpha^2\beta^4 + \alpha^4\beta^2\right)^{1/4}$.

In the limit $r \to \infty$, the function $q_{\rho,r}(d)$ converges to a Gaussian peak of width $\sim 1/\rho$. Since E must be positive, the $\tilde{f}(-E, -\mathbf{p})\langle E, \mathbf{p}|\psi_{i,\alpha}^{\dagger}(0)|\text{vac}\rangle$ term in (86) is exponentially small. Hence, one obtains

$$\langle E, \mathbf{p}|R|\text{vac}\rangle \simeq -i\lambda\tilde{f}(E, \mathbf{p})\langle E, \mathbf{p}|\psi_{i,\alpha}(0)|\text{vac}\rangle. \tag{90}$$

for $E \gg 1/\tau$ and $\lambda \ll 1$. By (90) and (27), one sees that $R|\text{vac}\rangle$ is a antifermion wavepacket with momentum centered around $\mathbf{p}$. To create a fermion, one interchanges ψ and $\psi^{\dagger}$ in (76).

Using the asymptotics of error functions, we can furthermore bound the contributions due to r being finite. One finds that

$$\left|q_{\rho,r}(d) - q_{\rho,\infty}(d)\right| \leq \frac{2}{r\rho^2}e^{-(\rho r)^2/4}. \tag{91}$$

4.4   Measuring Number Operators

Recall from §3.1 that the free theory ($g_0^2 = 0$) is exactly solvable, with the number operators $L^{-1}a_j^{\dagger}(\mathbf{p})a_j(\mathbf{p})$ counting fermions of species j in momentum-mode $\mathbf{p}$ and $L^{-1}b_j^{\dagger}(\mathbf{p})b_j(\mathbf{p})$ similarly counting antifermions. Thus, as one possible set of measurements to perform on the final state of the simulation, we propose, as in [8], adiabatically returning to the free theory and then measuring number operators via the phase-estimation algorithm. We analyze this measurement procedure in this section. An alternative set of measurements that is more suitable when bound states are present is analyzed in §4.5.

The adiabatic return to the free theory is performed in the presence of particle wavepackets, so the state being adiabatically transformed is not an energy eigenstate. Different energy eigenstates in the superposition will acquire different dynamical phases during the adiabatic process and thus, in physical terms, the simulated particles will propagate. Such propagation is undesirable because we do not want any scattering to occur while the interaction is being turned off.

Hence, we apply the same technique proposed in [8] to suppress particle propagation: we interleave (simulated) backwards time evolutions governed by time-independent Hamiltonians into the adiabatic process. By an analysis similar to that performed in [8], one finds that, to ensure that a particle propagates no further than a distance $\mathcal{D}$, it suffices to use

$$J = \widetilde{O}\left(\frac{\sqrt{\tau}}{p\mathcal{D}}\right) \tag{92}$$

backwards evolutions, where τ is the duration of the original adiabatic process and p is the momentum of the particle. Further, one finds that the total probability of diabatically exciting one or more particles is[4]

$$P_{\text{diabatic}} = O\left(\frac{J^2 L p^2}{\tau^2}\right). \tag{93}$$

Hence, setting $\mathcal{D}$ to a constant P_{diabatic} to ϵ, one obtains

$$\tau = \widetilde{O}\left(\frac{L}{\epsilon}\right). \tag{94}$$

---

[4]This result is based on the adiabatic criterion of [35] which appears to be applicable [8] to our Hamiltonian although it may not apply to all Hamiltonians.

A process of this duration can be implemented with (§3.3)

$$G_{\text{turn-off}} = O\left(\left(\frac{L^2}{a\epsilon}\right)^{1+o(1)}\right) \tag{95}$$

quantum gates.

The phase-estimation algorithm [36] enables one to measure in the eigenbasis of $L^{-1}a_j^\dagger(\mathbf{p})a_j(\mathbf{p})$, provided one can efficiently implement $e^{-iL^{-1}a_j^\dagger(\mathbf{p})a_j(\mathbf{p})t}$ for various t using quantum circuits. By (29) and (30), one sees that the problems of simulating $e^{-iL^{-1}a_j^\dagger(\mathbf{p})a_j(\mathbf{p})t}$ and its antifermionic counterpart are largely similar to the problem of simulating the time evolution e^{-iHt}, which was analyzed in detail in §3.3. However, these number operators are spatially nonlocal, which means that the methods of §3.3 do not perform well as a function of $\hat{L}$. Instead, it is more efficient to use recent techniques from [37].

In [37], a method is described for simulating sparse Hamiltonians in which the matrix elements are given by an oracle. As discussed on pg. 2 of [37], in the case where the sparse Hamiltonian consists of a sum of d terms each acting on $O(1)$ qubits, the number of oracle queries and non-oracle-related quantum gates both scale as $O(d)$. A number operator for a momentum mode consists of $O(\hat{L}^2)$ terms, acting between all pairs of spatial lattice sites. Thus, if one ignored the fermionic statistics, the number of non-oracle-related gates needed to simulate the time-evolution induced by a number operator would be $O(\hat{L}^2 n) = O(\hat{L}^3)$. The number of gates needed to implement one oracle query to the sparse matrix defined by the number operator would be $O(n)$, and number of quantum gates needed to implement all of the oracle queries would be $O(\hat{L}^3)$. Using the Bravyi-Kitaev encoding for fermionic statistics adds a logarithmic factor to the complexity. Measuring all $2N\hat{L}$ of the number operators thus has total complexity $\widetilde{O}(\hat{L}^4) = \widetilde{O}(L^4/a^4)$.

4.5 Measuring Local Charge

In previous work [8], we proposed measuring local energy observables as an alternative to returning to the free theory and measuring number operators. This procedure has the advantage that it can detect bound states. It has the disadvantage that the local energy observables have ultraviolet-divergent vacuum fluctuations that represent a noise background above which particle excitations must be discerned. In this paper, we instead measure simpler local observables, namely charges, whose vacuum fluctuations are less difficult to control. These observables can thus detect charged bound states, although they are blind to neutral ones.

From the equation of motion of the massive Gross-Neveu model, one finds that for each $j \in \{1, 2, \ldots, N\}$ the quantity

$$J_j^\mu(x) = \bar{\psi}_j(x)\gamma^\mu\psi_j(x) \tag{96}$$

obeys

$$\partial_\mu J_j^\mu = 0. \tag{97}$$

Hence,

$$\widetilde{Q}_j \equiv \sum_{\mathbf{x}} J_j^0(\mathbf{x}) = \sum_{\mathbf{x}} \bar{\psi}_j(\mathbf{x})\gamma^0\psi_j(\mathbf{x}) \tag{98}$$

is a conserved charge. Note that, for any $b, c \in \mathbb{R}$, $Q_j = b\widetilde{Q}_j + c$ is also conserved. We can calibrate the charge observable by demanding that the vacuum have zero charge and that particle creation

change the charge by ± 1. One satisfies these criteria with the following definition:

$$Q_j = \sum_{\mathbf{x}\in\Omega} a\bar{\psi}_j(\mathbf{x})\gamma^0\psi_j(\mathbf{x}) - \hat{L}\mathbb{1} . \tag{99}$$

By (27), (28), and (36), one finds that

$$Q_j = \frac{1}{L} \sum_{\mathbf{p}\in\Gamma} \left(a_j^\dagger(\mathbf{p})a_j(\mathbf{p}) - b_j^\dagger(\mathbf{p})b_j(\mathbf{p}) \right) . \tag{100}$$

For any envelope function $f : \Omega \to [0,1]$, one can similarly define

$$Q_j^{(f)} = \sum_{\mathbf{x}\in\Omega} f(\mathbf{x}) \left(a\bar{\psi}_j(\mathbf{x})\gamma^0\psi_j(\mathbf{x}) - \mathbb{1} \right) . \tag{101}$$

If f has support only in some region $R \subset \Omega$, then $Q_j^{(f)}$ can be thought of as an observable for the charge in that region.

The most obvious choice of f is a square function that is equal to one inside R and zero elsewhere. However, a better signal-to-noise ratio can be obtained by choosing f to decay from one to zero more smoothly at the boundary of R. Specifically, calculations (in Appendix A) show that, when f is chosen to be a Gaussian of width R, the variance of the observable $Q_j^{(f)}$ in the vacuum state is $O(1/mR)$, independent of the lattice spacing a. Hence the noise background above which particle excitations are to be detected is nondivergent in a and can be brought to an arbitrarily low level at the cost of increasing the detector size. In practice, one will use a truncated Gaussian, replacing the exponentially small tails with zero at distances greater than some constant multiple of R. This modified f then has support on a region of size $O(R)$, but the corresponding operator is exponentially close to the Gaussian case treated by our analysis.

$Q_j^{(f)}$ has eigenvalues with $O(1)$ separations. Thus, measuring $Q_j^{(f)}$ by phase estimation entails simulating the unitary transformation $\exp\left[iQ_j^{(f)}t\right]$ for t of order one. Because $Q_j^{(f)}$ is the sum of local terms, these unitary transformations can be implemented by techniques similar to those in §3.3 with complexity $O(a^{-1-o(1)}\epsilon^{-o(1)})$.

5 Some Field-Theoretical Aspects

This section describes some quantum field-theoretical calculations: analysis of the effect of discretizing the spatial dimension of the massive Gross-Neveu model, and the perturbative renormalization of the mass in the discretized theory.

In our complexity analysis (§2.3), our criterion for choosing the lattice spacing a is that the scattering cross sections for processes at a momentum scale p in the discretized theory should differ from their continuum values by at most a factor of $(1 + \epsilon)$. The results of §5.1 show that one can satisfy this criterion by choosing $a \sim \epsilon/p$. This choice then affects the overall scaling of the algorithm in the large-momentum and high-precision limits. As one would expect, higher energies and greater precision require a smaller lattice spacing and thus a larger number of lattice sites (for fixed L). Consequently, the number of quantum gates needed to simulate time evolutions via Suzuki-Trotter formulae is larger.

In §5.2, we perturbatively calculate the relationship between the bare mass m_0, which is a parameter in the lattice Hamiltonian (see (22) and (23)), and the physical mass m of the particles

in the theory. We need to know the behavior of m in order to design and analyze the procedure for preparing the interacting vacuum (§4.2). In particular, a suitable adiabatic path must maintain a non-zero mass, the magnitude of which affects the algorithmic complexity, as indicated by the adiabatic theorem.

5.1 Effects of Non-zero Lattice Spacing

The effects of a non-zero lattice spacing can be analyzed via effective field theory. The discretized Lagrangian can be thought of as the leading contribution to an effective field theory, neglected terms of which correspond to discretization errors. Hence, the scaling of the error with the lattice spacing is given by the scaling of the coefficients of those terms.

The symmetries of the continuum theory restrict the possible operators in the effective field theory. Consider the discrete transformations parity (denoted P), time reversal (T), and charge conjugation (C). Parity changes the handedness of space and hence reverses the momentum. Thus,

$$Pa(\mathbf{p})P = a(-\mathbf{p}), \qquad Pb(\mathbf{p})P = -b(-\mathbf{p}). \tag{102}$$

Using (4) and (102), we then obtain

$$P\psi(t, \mathbf{x})P = \gamma^0 \psi(t, -\mathbf{x}), \qquad P\bar{\psi}(t, \mathbf{x})P = \bar{\psi}(t, -\mathbf{x})\gamma^0. \tag{103}$$

Likewise,

$$Ta(\mathbf{p})T = a(-\mathbf{p}), \qquad Tb(\mathbf{p})T = -b(-\mathbf{p}). \tag{104}$$

It turns out that time reversal needs to be an antilinear operator. Then

$$T\psi(t, \mathbf{x})T = \gamma^1 \psi(-t, \mathbf{x}), \qquad T\bar{\psi}(t, \mathbf{x})T = -\bar{\psi}(-t, \mathbf{x})\gamma^1. \tag{105}$$

Finally, charge conjugation interchanges particles and antiparticles. Thus,

$$Ca(\mathbf{p})C = b(\mathbf{p}), \qquad Cb(\mathbf{p})C = a(\mathbf{p}), \tag{106}$$

and

$$C\psi(t, \mathbf{x})C = \psi^*(t, \mathbf{x}), \qquad C\bar{\psi}(t, \mathbf{x})C = \psi^T(t, \mathbf{x})\gamma^0. \tag{107}$$

One can verify that the Lagrangian (2) is invariant under each of the transformations P, T and C.

Now consider the operator $\psi^\dagger \mathbb{M}\psi$, where $\mathbb{M}$ is Hermitian. Invariance under P, T and C requires

$$\mathbb{M} = \gamma^0 \mathbb{M}\gamma^0, \tag{108}$$
$$\mathbb{M} = -\gamma^1 \mathbb{M}^* \gamma^1, \tag{109}$$
$$\mathbb{M} = -\mathbb{M}^T. \tag{110}$$

These conditions imply that

$$\mathbb{M} = c\gamma^0, \ c \in \mathbb{R}. \tag{111}$$

Likewise, for $i\psi^\dagger \mathbb{M}\partial_\mu \psi$, where $\mathbb{M}$ is Hermitian, P, T and C invariance requires

$$\mathbb{M} = (-1)^\mu \gamma^0 \mathbb{M}\gamma^0, \tag{112}$$
$$\mathbb{M} = -(-1)^\mu \gamma^1 \mathbb{M}^* \gamma^1, \tag{113}$$
$$\mathbb{M} = \mathbb{M}^T. \tag{114}$$

These conditions imply that, for $\mu = 0$,

$$\mathbb{M} = c\mathbb{1} = c(\gamma^0)^2\,, \quad c \in \mathbb{R}\,, \tag{115}$$

while, for $\mu = 1$,

$$\mathbb{M} = c\gamma^5 = -c\gamma^0\gamma^1\,, \quad c \in \mathbb{R}\,. \tag{116}$$

Thus, the only P-, T- and C-invariant bilinears of Dirac fields are $\bar\psi\psi$ and $i\bar\psi\gamma^\mu\partial_\mu\psi$ ($\mu = 0$ or 1).

Now consider four-fermion operators, namely, products of two bilinears. The set $\{\mathbb{1}, \sigma^i\}$ forms a complete basis, elements of which satisfy the identity

$$\delta_{\alpha\beta}\delta_{\gamma\delta} \;=\; \frac{1}{2}\big(\delta_{\alpha\delta}\delta_{\gamma\beta} + \sum_{i=1}^{3}\sigma^i_{\alpha\delta}\sigma^i_{\gamma\beta}\big)\,. \tag{117}$$

For $\gamma^0 = \sigma^2$, $\gamma^1 = -i\sigma^1$, $\gamma^5 = \sigma^3$, this is equivalent to

$$\delta_{\alpha\beta}\delta_{\gamma\delta} \;=\; \frac{1}{2}(\delta_{\alpha\delta}\delta_{\gamma\beta} + (\gamma^\mu)_{\alpha\delta}(\gamma_\mu)_{\gamma\beta} + (\gamma^5)_{\alpha\delta}(\gamma^5)_{\gamma\beta})\,. \tag{118}$$

Equation (118) can be used to obtain Fierz identities. For example,

$$\begin{aligned}
\bar\psi_i\psi_j\bar\psi_j\psi_i &= (\bar\psi_i)_\alpha(\psi_j)_\beta(\bar\psi_j)_\gamma(\psi_i)_\delta\delta_{\alpha\beta}\delta_{\gamma\delta} \\
&= -\frac{1}{2}\big(\bar\psi_i\psi_i\bar\psi_j\psi_j + \bar\psi_i\gamma^\mu\psi_i\bar\psi_j\gamma_\mu\psi_j + \bar\psi_i\gamma^5\psi_i\bar\psi_j\gamma^5\psi_j\big)\,,
\end{aligned} \tag{119}$$

where the minus sign comes from fermion anticommutation. Thus, any operator of the form $\bar\psi_i\tilde\Gamma_1\psi_j\bar\psi_j\tilde\Gamma_2\psi_i$ can be rewritten as a sum of operators of the form $\bar\psi_i\Gamma_1\psi_i\bar\psi_j\Gamma_2\psi_j$, with $\Gamma_{1,2} \in \{\mathbb{1}, \gamma^\mu, \gamma^5\}$.

If $\Gamma_1 \neq \Gamma_2$, then $\bar\psi_i\Gamma_1\psi_i\bar\psi_j\Gamma_2\psi_j$ will violate at least one of the discrete symmetries. Furthermore, the $O(N)$ symmetry[5] associated with the N fermion species restricts the allowed form of operators to functions of $\sum_{i=1}^{N}\bar\psi_i\Gamma\psi_i$. For $i \neq j$, $\bar\psi_i\gamma^5\psi_i\bar\psi_j\gamma^5\psi_j$ is ruled out by invariance under P (or C) of any single field ψ_i, and thus $\big(\sum_{i=1}^{N}\bar\psi_i\gamma^5\psi_i\big)^2$ is ruled out. Likewise, $\bar\psi_i\gamma^\mu\psi_i\bar\psi_j\gamma_\mu\psi_j$ ($i \neq j$) and consequently $\big(\sum_{i=1}^{N}\bar\psi_i\gamma^5\psi_i\big)^2$ are ruled out.

We conclude that the only four-fermion operator (without derivatives) in the effective field theory is $\big(\sum_{i=1}^{N}\bar\psi_i\psi_i\big)^2$.

Each extra derivative or factor of $\bar\psi\Gamma\psi$ in an operator will increase its mass dimension by one; correspondingly, it will be suppressed by an extra power of a. We therefore conclude that no new unsuppressed operators are induced in the effective field theory. The spatial derivative in the continuum theory is approximated by a difference operator, with an error of order a, and the Wilson term is also formally of order a. Spatial discretization errors are hence of order a.

5.2 Mass Renormalization

In this subsection, we calculate the renormalized (or physical) mass of the discretized theory, using second-order perturbation theory. A convenient way to obtain a suitable expression is to use a partially renormalized form of perturbation theory (as was done in [8]), in which one uses the bare coupling but the renormalized mass.

---

[5]In fact, the massive Gross-Neveu model has an $O(2N)$ symmetry.

To perform perturbative calculations, we need the Feynman rules for the discretized theory. The propagator is

$$\longrightarrow \quad = \frac{\gamma^\mu \tilde{p}_\mu + \widetilde{m}(p)}{\tilde{p}^2 - \widetilde{m}(p)^2}, \tag{120}$$

where

$$\tilde{p}^\mu = \left(p^0, \frac{1}{a}\sin(ap^1)\right), \qquad \widetilde{m}(p) = m + \frac{2r}{a}\sin^2\left(\frac{ap^1}{2}\right). \tag{121}$$

For convenience, we use the standard technique of introducing an auxiliary field σ and rewrite the Lagrangian as

$$\mathcal{L} = \mathcal{L}_0 + \mathcal{L}_\sigma, \tag{122}$$

where $\mathcal{L}_0$ is the discretized free Lagrangian and

$$\mathcal{L}_\sigma = -\frac{1}{2}\sigma^2 - g\sigma\bar{\psi}_j\psi_j. \tag{123}$$

The corresponding Feynman rules are

$$\cdots\cdots\cdots = -i, \qquad \rangle\cdots = -ig. \tag{124}$$

At one-loop order,

$$-iM(p) \quad = \quad \overparen{\cdot\!\!-\!\!\cdot} \quad + \quad \!\!-\!\!\otimes\!\!-\!\! \quad, \tag{125}$$

where the second diagram is the counterterm.

The first diagram gives

$$\overparen{\cdot\!\!-\!\!\cdot} \quad = \quad -g_0^2 \int_{-\infty}^{\infty} \frac{dk^0}{2\pi} \int_{-\pi/a}^{\pi/a} \frac{dk^1}{2\pi} \frac{\gamma^\mu \tilde{k}_\mu + \widetilde{m}(k)}{\tilde{k}^2 - \widetilde{m}(k)^2} \tag{126}$$

$$= \quad \frac{ig_0^2}{4\pi a} \int_{-\pi}^{\pi} dk^1 \frac{ma + 2r\sin^2\left(\frac{k^1}{2}\right)}{\sqrt{\sin^2 k^1 + \left(ma + 2r\sin^2\left(\frac{k^1}{2}\right)\right)^2}}. \tag{127}$$

The term in (127) proportional to r scales as $1/a$ and gives the mass correction to the doubler (spurious fermion). The term proportional to m gives the following:

$$m_0 = m - \frac{g_0^2 m}{2\pi}\log(ma) + \cdots. \tag{128}$$

At two-loop order, the 1PI amplitude has the additional contributions

$$\overparen{\cdot\!\!-\!\!\cdot} \quad + \quad \overparen{\cdot\otimes\cdot} \quad + \quad \overparen{\cdot\!\!-\!\!\cdot} \quad + \quad \overparen{\cdot\diamond\cdot} \quad.$$

The renormalization condition satisfied at first order implies that the first two diagrams cancel.

The last two diagrams give

$$\overparen{\cdot\!\!-\!\!\cdot} \quad = \quad -\frac{ig_0^4}{16\pi^3}\left(mI_1^{(a)} + \frac{1}{a}I_1^{(b)}\right) \tag{129}$$

24

and

$$\text{(diagram)} = \frac{ig_0^4 N}{16\pi^3}\left(mI_2^{(a)} + \frac{1}{a}I_2^{(b)}\right), \tag{130}$$

where $I_1^{(a)}$, $I_1^{(b)}$, $I_2^{(a)}$ and $I_2^{(b)}$ are given in Appendix B. Numerical evaluation of these integrals reveals the forms

$$I_i^{(b)} = c^{(b1)} - c^{(b2)} ma + \cdots, \tag{131}$$

$$I_i^{(a)} = c_i^{(a1)} \log^2(ma) - c_i^{(a2)} \log(ma) + c_i^{(a3)} + \cdots, \tag{132}$$

with $c_i^{(j)} > 0$. We thus obtain

$$m = m^{(1)} - \frac{g_0^4 m^{(1)}}{16\pi^3}\left(Nc_2^{(a1)} - c_1^{(a1)}\right)\log^2(m^{(1)}a) + \cdots, \tag{133}$$

where $m^{(1)}$ denotes the physical mass at one-loop order.

A   Variance of Local Charge

Consider $\widetilde{Q}_j^{(f)}$ in the continuum limit:

$$\widetilde{Q}_j^{(f)} = \int dx \, J_j^{(0)}(\mathbf{x}) f(\mathbf{x}) \,. \tag{134}$$

We wish to compute its variance, which is given by

$$\left\langle (\widetilde{Q}_j^{(f)} - \langle \widetilde{Q}_j^{(f)} \rangle)^2 \right\rangle = \int dx \, dy \, f(\mathbf{x}) f(\mathbf{y}) \big(\langle J_j^{(0)}(\mathbf{x}) J_j^{(0)}(\mathbf{y}) \rangle - \langle J_j^{(0)}(\mathbf{x}) \rangle \langle J_j^{(0)}(\mathbf{y}) \rangle \big) \tag{135}$$

$$= \int \frac{d^2 k}{(2\pi)^2} |\widetilde{f}(k)|^2 \widetilde{G}_c(k) \,, \tag{136}$$

where G_c is the connected Green's function. By standard quantum field-theoretical methods, we obtain

$$\widetilde{G}_c(k^0, k^1) = 2i \int_0^1 dx \int \frac{d^2 p_E}{(2\pi)^2} \frac{m^2 - x(1-x)((k^0)^2 + (k^1)^2)}{[p_E^2 + m^2 - x(1-x)((k^0)^2 - (k^1)^2)]^2} \,, \tag{137}$$

$$= \frac{i}{2\pi} \int_0^1 dx \, \frac{m^2 - x(1-x)((k^0)^2 + (k^1)^2)}{m^2 - x(1-x)((k^0)^2 - (k^1)^2)} \,. \tag{138}$$

Substituting $\widetilde{G}_c$ into (136) and using an ultraviolet regulator, we obtain

$$\left\langle (\widetilde{Q}_j^{(f)} - \langle \widetilde{Q}_j^{(f)} \rangle)^2 \right\rangle = \frac{1}{(2\pi)^2} \int dk_1 |\widetilde{f}(k^1)|^2 \int_0^1 dx \, \frac{(k^1)^2}{\sqrt{(k^1)^2 + \frac{m^2}{x(1-x)}}} \,. \tag{139}$$

For the square window function $f(x) = \theta(R/2 - |x|)$, the charge fluctuation diverges, but only logarithmically, with

$$\left\langle (\widetilde{Q}_j^{(f)} - \langle \widetilde{Q}_j^{(f)} \rangle)^2 \right\rangle \leq \frac{2}{\pi^2} \big(\log(2\pi) - 1 - \log(ma) \big) + O((ma)^2) \,. \tag{140}$$

For $f(x) = \exp(-x^2/R^2)$,

$$\left\langle (\widetilde{Q}_j^{(f)} - \langle \widetilde{Q}_j^{(f)} \rangle)^2 \right\rangle = \frac{\sqrt{2}\pi^{3/2}}{32} \frac{1}{mR} + \dots \,. \tag{141}$$

B Integrals for Mass Renormalization

For $i = 1, 2$,

$$I_i^{(a)} = \iiint_0^1 dx\, dy\, dz\, \frac{\delta(x+y+z-1)}{\sqrt{xy+xz+yz}} \int_{-\pi}^{\pi} dk \int_{-\pi}^{\pi} dq \left(\frac{N_i^{(a1)}}{2(xy+xz+yz)^2 D} + \frac{N_i^{(a2)}}{D^2} \right), \quad (142)$$

$$I_i^{(b)} = r \iiint_0^1 dx\, dy\, dz\, \frac{\delta(x+y+z-1)}{\sqrt{xy+xz+yz}} \int_{-\pi}^{\pi} dk \int_{-\pi}^{\pi} dq \left(\frac{N_i^{(b1)}}{2(xy+xz+yz)^2 D} + \frac{N_i^{(b2)}}{D^2} \right), \quad (143)$$

where

$$D = x\left[\sin^2(k) + \left(ma + 2r\sin^2\left(\frac{k}{2}\right) \right)^2 \right] + y\left[\sin^2(q) + \left(ma + 2r\sin^2\left(\frac{q}{2}\right) \right)^2 \right] \tag{144}$$

$$+ z\left[\sin^2(q-k) + \left(ma + 2r\sin^2\left(\frac{q-k}{2}\right) \right)^2 \right] - \frac{xyz}{xy+xz+yz}(ma)^2,$$

$$N_1^{(a1)} = x^2 y - xy^2 + x^2 z + 4xyz - y^2 z + xz^2 + yz^2, \tag{145}$$

$$N_1^{(a2)} = 4f_3 r^2 \sin^2\left(\frac{k}{2}\right) \sin^2\left(\frac{k-q}{2}\right) + f_3 \sin(k)\sin(k-q) + 4f_2 r^2 \sin^2\left(\frac{k}{2}\right) \sin^2\left(\frac{q}{2}\right) \tag{146}$$

$$+ 4f_1 r^2 \sin^2\left(\frac{k-q}{2}\right) \sin^2\left(\frac{q}{2}\right) - f_2 \sin(k)\sin(q) + f_1 \sin(k-q)\sin(q)$$

$$+ 2(ma)r\left(f_2 f_3 \sin^2\left(\frac{k}{2}\right) + f_1 f_3 \sin^2\left(\frac{k-q}{2}\right) + f_1 f_2 \sin^2\left(\frac{q}{2}\right) \right) + (ma)^2 f_1 f_2 f_3,$$

$$f_1 = \frac{xy+xz+2yz}{xy+xz+yz}, \qquad f_2 = \frac{2xy+xz+yz}{xy+xz+yz}, \qquad f_3 = \frac{xy+xz}{xy+xz+yz},$$

$$N_1^{(b1)} = x^2 y - xy^2 + x^2 z + xyz - y^2 z + xz^2 + yz^2 \tag{147}$$

$$- (xy+xz+yz)(x\cos(k) - y\cos(q) + z\cos(k-q)),$$

$$N_1^{(b2)} = 8r^2 \sin^2\left(\frac{k}{2}\right) \sin^2\left(\frac{k-q}{2}\right) \sin^2\left(\frac{q}{2}\right) + 2\sin(k)\sin(k-q)\sin^2\left(\frac{q}{2}\right) \tag{148}$$

$$- 2\sin(k)\sin^2\left(\frac{k-q}{2}\right)\sin(q) + 2\sin^2\left(\frac{k}{2}\right)\sin(k-q)\sin(q),$$

$$N_2^{(a1)} = 4z(xy+xz+yz), \tag{149}$$

$$N_2^{(a2)} = -(ma)^2 \frac{(xyz)^2}{(xy+xz+yz)^3} - (ma)\frac{xyz^2\left(ma + 2r\sin^2\left(\frac{k-q}{2}\right) \right)}{(xy+xz+yz)^2} \tag{150}$$

$$+ \frac{2xy+xz+yz}{xy+xz+yz}\left(\left(ma + 2r\sin^2\left(\frac{k}{2}\right) \right)\left(ma + 2r\sin^2\left(\frac{q}{2}\right) \right) - \sin(k)\sin(q) \right)$$

$$+ 2r\sin^2\left(\frac{k-q}{2}\right)\left(ma + 2r\left(\sin^2\left(\frac{k}{2}\right) + \sin^2\left(\frac{q}{2}\right) \right) \right),$$

$$N_2^{(b1)} = 2z(xy+xz+yz)\sin^2\left(\frac{k-q}{2}\right), \tag{151}$$

$$N_2^{(b2)} = 2\sin^2\left(\frac{k-q}{2}\right)\left(4r^2 \sin^2\left(\frac{k}{2}\right)\sin^2\left(\frac{q}{2}\right) - \sin(k)\sin(q) \right). \tag{152}$$

References

[1] Seth Lloyd, *Universal quantum simulators*, Science **273** (1996), 1073–1078.

[2] Daniel S. Abrams and Seth Lloyd, *Simulation of many-body Fermi systems on a universal quantum computer*, Physical Review Letters **79** (1997), 2586–2589.

[3] Christof Zalka, *Efficient simulation of quantum systems by quantum computers*, Proc. R. Soc. London Ser. A **454** (1998), 313–322.

[4] B. P. Lanyon, C. Hempel, D. Nigg, M. Müller, R. Gerritsma, F. Zähringer, P. Schindler, J. T. Barreiro, M. Rambach, G. Kirchmair, M. Hennrich, P. Zoller, R. Blatt, and C. F. Roos, *Universal digital quantum simulation with trapped ions*, Science **334** (2011), 57.

[5] M. Müller, K. Hammerer, Y. L. Zhou, C. F. Roos, and P. Zoller, *Simulating open quantum systems: from many-body interactions to stabilizer pumping*, New J. Phys. **13** (2011), 085007.

[6] Julio T. Barreiro, Markus Müller, Philipp Schindler, Daniel Nigg, Thomas Monz, Michael Chwalla, Markus Hennrich, Christian F. Roos, Peter Zoller, and Rainer Blatt, *An open-system quantum simulator with trapped ions*, Nature **470** (2011), 486–491.

[7] Stephen P. Jordan, Keith S. M. Lee, and John Preskill, *Quantum algorithms for quantum field theories*, Science **336** (2012), 1130–1133. arXiv:1111.3633.

[8] ———, *Quantum computation of scattering in scalar quantum field theories*, Quantum Information and Computation **14** (2014), 1014–1080. arXiv:1112.4833.

[9] Sergey B. Bravyi and Alexei Yu. Kitaev, *Fermionic quantum computation*, Annals of Physics **298** (2002), 210–226. arXiv:quant-ph/0003137.

[10] Uwe-Jens Wiese, *Ultracold quantum gases and lattice systems: quantum simulation of lattice gauge theories*, Annalen der Physik **525** (2013), no. 10–11, 777–796. arXiv:1305.1602.

[11] J. Beringer et al., *Review of particle physics*, Physical Review D **86** (2012), 010001.

[12] David J. Gross and André Neveu, *Dynamical symmetry breaking in asymptotically free field theories*, Physical Review D **10** (1974), 3235.

[13] Roger F. Dashen, Brosl Hasslacher, and André Neveu, *Semiclassical bound states in an asymptotically free theory*, Physical Review D **12** (1975), 2443.

[14] Kazushige Machida and Hiizu Nakanishi, *Superconductivity under a ferromagnetic molecular field*, Physical Review B **30** (1984), 122–133.

[15] Hsiu-Hau Lin, Leon Balents, and Matthew P. A. Fisher, *Exact SO(8) symmetry in the weakly-interacting two-leg ladder*, Physical Review B **58** (1998), 1794–1825.

[16] A. Neveu and N. Papanicolaou, *Integrability of the classical $[\bar{\varphi}_i \varphi_i]_2^2$ and $[\bar{\varphi}_i \varphi_i]_2^2 - [\bar{\varphi}_i \gamma_5 \varphi_i]_2^2$ interactions*, Communications in Mathematical Physics **58** (1978), 31.

[17] N. Andrei and J. H. Lowenstein, *Diagonalization of the chiral invariant Gross-Neveu Hamiltonian*, Physical Review Letters **43** (1979), 1698–1701.

[18] E. Brézin, C. Itzykson, J. Zinn-Justin, and J.-B. Zuber, *Remarks about the existence of nonlocal charges in two-dimensional models*, Physics Letters B **82** (1979), 442–444.

[19] Alexander B. Zamolodchikov and Alexei B. Zamolodchikov, *Factorized S-matrices in two dimensions as the exact solutions of certain relativistic quantum field theory models*, Annals of Physics **120** (1979), 253–291.

[20] M. Karowski and H. J. Thun, *Complete S-matrix of the O(2N) Gross-Neveu model*, Nuclear Physics **B190** (1981), 61.

[21] Joshua Feinberg and A. Zee, *Fermion bags in the massive Gross-Neveu model*, Physics Letters B **411** (1997), 134–140. hep-th/9610009.

[22] J. Feldman, J. Magnen, V. Rivasseau, and R. Sénéor, *Massive Gross-Neveu model: A rigorous perturbative construction*, Physical Review Letters **54** (1985), 1479–1481.

[23] —————, *A renormalizable field theory: The massive Gross-Neveu model in two dimensions*, Communications in Mathematical Physics **103** (1986), 67–103.

[24] M. Suzuki, *Fractal decomposition of exponential operators with applications to many-body theories and Monte Carlo simulations*, Physics Letters A **146** (1990), 319–323.

[25] A. Y. Kitaev, *Quantum computations: algorithms and error correction*, Russian Mathematical Surveys **52** (1997), 1191–1249.

[26] Christopher M. Dawson and Michael A. Nielsen, *The Solovay-Kitaev algorithm*, Quantum Information and Computation **6** (2006), 81–95. arXiv:quant-ph/0505030.

[27] Kenneth G. Wilson, *Confinement of quarks*, Physical Review D **10** (1974), 2445–2459.

[28] P. Jordan and E. P. Wigner, *Über das Paulische äquivalenzverbot*, Zeitschrift für Physik **47** (1928), 631–651.

[29] Masuo Suzuki, *General decomposition theory of ordered exponentials*, Proceedings of the Japan Academy, Series B **69** (1993), 161–166.

[30] Nathan Wiebe, Dominic W. Berry, Peter Høyer, and Barry C. Sanders, *Higher order decompositions of ordered operator exponentials*, Journal of Physics A **43** (2010), 065203. arXiv:math-ph/0812.0562.

[31] D. W. Berry, G. Ahokas, R. Cleve, and B. C. Sanders, *Efficient quantum algorithms for simulating sparse Hamiltonians*, Communications in Mathematical Physics **270** (2007), 359–371. arXiv:quant-ph/0508139.

[32] Sadegh Raeisi, Nathan Wiebe, and Barry C. Sanders, *Quantum-circuit design for efficient simulations of many-body quantum dynamics*, New Journal of Physics **14** (2012), 103017.

[33] Sabine Jansen, Ruedi Seiler, and Mary-Beth Ruskai, *Bounds for the adiabatic approximation with applications to quantum computation*, Journal of Mathematical Physics **48** (2007), 102111. arXiv:quant-ph/0603175.

[34] Jeffrey Goldstone, *Adiabatic theorem*. Recounted in Appendix F of arXiv:0809.2307.

[35] Albert Messiah, *Quantum mechanics*, Dover, 1999. (Reprint of the two-volume edition published by Wiley, 1961-1962).

[36] A. Yu Kitaev, *Quantum measurements and the Abelian stabilizer problem*, arXiv:quant-ph (1995).

[37] Dominic W. Berry, Andrew M. Childs, Richard Cleve, Robin Kothari, and Rolando D. Somma, *Exponential improvement in precision for simulating sparse Hamiltonians*, arXiv:1312.1414 (2013).